Published in final edited form as:
Cancer Res. 2010 May 1; 70(9): 3566–3575. doi:10.1158/0008-5472.CAN-09-3219.

YPEL3, a p53-regulated gene that induces cellular senescence

Kevin Kelley[1,2], **Kelly R. Miller**[1,2], **Amber Todd**[1], **Amy Kelley**[1], **Rebecca Tuttle**[3], and **Steven J. Berberich**[1]

[1] Wright State University Biochemistry & Molecular Biology Department 3640 Colonel Glenn Highway. Dayton, OH 45435

[3] Wright State University Department of Surgery 1 Wyoming St. Dayton, OH 45409

Abstract

Cellular senescence, the limited ability of cultured normal cells to divide, can result from cellular damage triggered through oncogene activation (premature senescence) or the loss of telomeres following successive rounds of DNA replication (replicative senescence). While both processes require a functional p53 signaling pathway, relevant downstream p53 targets have been difficult to identify. Discovery of senescence activators is important because induction of tumor cell senescence may represent a therapeutic approach for the treatment of cancer. In microarray studies where p53 was reactivated in MCF7 cells, we discovered that YPEL3 (Yippee-like-3), a member of a recently discovered family of putative zinc finger motif coding genes consisting of YPEL1-5, is a p53-regulated gene. YPEL3 expression induced by DNA damage leads to p53 recruitment to a cis-acting DNA response element located near the human YPEL3 promoter. Physiological induction of YPEL3 results in a substantial decrease in cell viability associated with an increase in cellular senescence. Through the use of RNAi and H-ras induction of cellular senescence, we demonstrate that YPEL3 activates cellular senescence downstream of p53. Consistent with its growth suppressive activity, YPEL3 gene expression is repressed in ovarian tumor samples. One mechanism of YPEL3 downregulation in ovarian tumor cell lines appears to be hypermethylation of a CpG island upstream of the YPEL3 promoter. We believe these findings point to YPEL3 being a novel tumor suppressor, which upon induction triggers a permanent growth arrest in human tumor and normal cells.

Keywords

YPEL3; p53; senescence; Ras; shRNA; SUAP

Introduction

Biochemical and genetic data demonstrate that in response to a variety of cellular stresses, the p53 tumor suppressor protein plays a critical role in the inhibition of cell proliferation. While p53 can elicit transcription-independent apoptosis (1), it also functions as a transcription factor inducing genes and miRNAs to mediate its complex biological functions (2). While p53 transcriptional and non-transcriptional mechanisms to induce apoptosis have been linked to tumor inhibition (3), recent *in vivo* studies have demonstrated that p53-dependent cellular senescence represents an important mechanism to block tumor development (4,5). These findings suggest that studies focused on understanding signaling pathways in senescence may lead to new targets.

Correspondence to: Steven J. Berberich.

[2]These authors contributed equally.

It is known that p53 and Rb signaling pathways are at the nexus of senescence resulting from oncogene activation (premature senescence) or telomere shorting (replicative senescence) (6). However, unlike apoptosis and transient cell cycle arrest, less is known about the p53 targets critical to cellular senescence. While it is accepted that cyclin-dependent kinase inhibitor and p53-target gene p21 is induced as cells undergo senescence, in some cell systems, loss of p21 leads to senescence bypass (7); yet in other cell systems, p21-null cells can still undergo a ras-mediated senescence (8). In contrast to p21, plasminogen-activator inhibitor 1 (PAI-1) represents a critical p53-regulated gene in cellular senescence of both murine and human cells (9).

In studies where we triggered a p53-dependent cell cycle arrest in MCF7 cells through RNAi targeting of HdmX or Hdm2, both p53 negative regulators, we uncovered several novel p53-regulated genes, one of which was YPEL3 (10). Located on the short arm of chromosome 16, YPEL3 is part of a five member family of closely related paralogues—YPEL1-5 that are named in reference to their *Drosophila* orthologue (11). The *Drosophila* Yippee protein was identified as a putative zinc-finger-motif containing protein with a high degree of conservation among the cysteines and histidines which form the motif (12).

Murine YPEL3 has been demonstrated to have an association with the induction of cell growth inhibition through apoptosis. Originally named SUAP for small unstable apoptotic protein, murine YPEL3 was linked to apoptosis in a screen for genes involved in programmed cell death of murine myeloid precursor (MMP) cells during differentiation (13).

In the present study we set out to examine whether the human YPEL3 gene was a novel p53 transcriptional gene target. Using DNA damage, chromatin immunoprecipitation and luciferase reporter assays we show that YPEL3 is regulated by p53. In assessing the biological activity of YPEL3 we demonstrate that it encodes a protein that induces cellular senescence in human tumor and normal cells. Consistent with this growth suppressive activity YPEL3 is seen downregulated in ovarian tumor samples. Using ovarian tumor cell lines we observed that CpG hypermethylation appears to be one mechanism by which YPEL3 gene expression is suppressed. Overall these studies identify YPEL3 as a p53-dependent, tumor suppressor gene.

Materials and Methods

YPEL3 expression plasmids

The tetracycline-inducible (tet-on) lentiviral YPEL3- V5-tagged expression construct was designed by cloning the YPEL3 ORF into pENTR/SD/D-TOPO and then into the pLenti4-T/O-V5 DEST vector via the Gateway cloning system (Invitrogen).

RT-PCR

Total RNA was isolated using the e.Z.N.A. Total RNA kit (Omega Bio-Tek) according to the manufacturer's instructions. RNA quality and quantity was assessed on a RNA nanochip (Agilent Technologies). One microgram of total RNA was used as a template for cDNA synthesis using the reverse transcriptase core reagent kit (Applied Biosystems). Taqman based PCR was performed in triplicate using Assay on Demand probe sets (Applied Biosystems) and an Applied Biosystems 7900 Sequence Detection System. GAPDH was used as an endogenous control. All Assay on Demand probes used in these experiments (YPEL3, p21, Bax and GAPDH) were validated gene targets.

Cell Lines

H1299 cells are derived from non-small-cell lung carcinoma devoid of p53. U2OS osteosarcoma cells, HepG2 hepatocarcinoma and MCF7 breast carcinoma cells all express

wild-type p53. HCT116 +/+ and -/- p53 colon carcinoma cell lines are isogenic with the exception of p53 status. IMR90 cells are primary human diploid fibroblasts. All of these cell lines were purchased from the American Type Culture Collection. 76ntert immortalized mammary epithelial cells also express wild-type p53 and were a generous gift from Dr. Vimla Band (University of Nebraska). A2780, Cp70 and C30 cell lines were obtained from Dr. Hamilton (Fox Chase). A2780 cells express wild-type p53, whereas Cp70 and C30 cells are p53 null or mutated, respectively. All cell line passages in these experiments were grown for no longer than three months.

DNA Damage Experiments

Twenty-four hours prior to treatment, 76ntert immortalized mammary epithelial cells were seeded at a density of 150k-cells/6cm plate. The following day the plates were treated with increasing doses of bleomycin or doxorubicin. Twenty-four hours later cells were harvested. Total RNA was extracted from the harvested cells and gene expression analyzed by RT-PCR.

Reporter Assays

The YPEL3-luc reporter plasmid contains -1386 to +120 of the YPEL3 promoter region (+1 representing the transcriptional start site) cloned in front of the luciferase gene in pGL3-Basic. The YPEL3(-485:+120) reporter plasmid contains -485 to +120 of the YPEL3 promoter cloned into pGL3-Basic. A 50 bp region of the YPEL3 promoter (Figure 2D), a triple mutant (containing mutations to the critical nucleotides in each half-site), and a randomly generated scramble sequence were cloned into pGL3-Basic. H1299 cells were plated at 60k cells per well in 12 well plates 24 hours prior to cotransfection with the indicated expression and luciferase vectors. The following day, cells were lysed on the plate using 1X passive lysis buffer (Promega) and analyzed by Dual Luciferase Assay Kit (Promega) according to the manufacturer's instructions. The experimental reporter's luciferase activity was normalized to *renilla* luciferase activity measured in relative light units. All experiments for each treatment were performed in triplicate. Error bars show variation as the standard deviation of each set of biological triplicates. Statistical significance was determined by using the paired student's t-test (Sigma Plot, p-value <0.05).

Immunoblotting

Whole cell extracts and Western blotting were performed as previously described with the following modifications (14). Cell pellets were lysed in three freeze-thaws using single lysis buffer (50mM Tris, pH 8.0, 150mM NaCl, 1% NP40) containing a protease inhibitor cocktail (Sigma). For endogenous YPEL3 and p53 Westerns, 10-20% gradient Tricine gels were used to separate 100 micrograms of protein extract. Proteins were transferred to PVDF using a semi-dry transfer apparatus (Fisher Biotech). Antibodies were obtained from Proteintech (YPEL3) and Calbiochem (p53, Ab-4 and Ab-6).

Chromatin Immunoprecipitation

Chromatin immunoprecipitation (ChIP) of the YPEL3 promoter region was performed using the ChIP-It Express Chromatin Immunoprecipitation kit (Active Motif) according to the manufacturer's instructions. Briefly, six 15 cm culture plates of HCT116 cells expressing wild-type p53 were grown to 70% confluence after which doxorubicin (0.3 μg/mL) was applied to three plates. Following a twenty hour incubation the cells were fixed in formaldehyde and sonicated to average chromatin fragments of 300-500 bps. Overnight incubation of chromatin-protein crosslinked complexes with either 2 μg p53 DO-1 antibody or an equivalent amount of normal mouse IgG (Santa Cruz) and 50 μL of magnetic bead slurry (Active Motif) was carried out for each sample. PCR of enriched chromatin was performed using GoTAQ master mix (Promega). PCR cycling parameters used are as follows: an initial denaturation step at 95°

C for two minutes followed by 36-40 cycles at 95°C for 30 seconds, 55°C for 30 seconds and 72°C for 40 seconds with a final extension time of five minutes. Primers used will be provided upon request.

Lentiviral Production and Colony Formation Assay

Lentivirus was produced by cotransfection of 293FT cells with a pLenti vector and lentiviral packaging mix (Invitrogen) according to the manufacturer's instructions. Lentivirus-containing supernatant was harvested at 48 hours post transfection, purified by centrifugation and stored at -80°C. MCF7 and U2OS cells containing Tetracycline Repressor (100,000 cells/well) were transduced with Lenti-YPEL3 or left untreated followed by incubation in complete medium for 24 hours. Infections were carried out overnight in the presence of 4 μg/mL Polybrene (Sigma). Following transductions, cells were selected with 750 μg/mL and 500 μg/mL Zeocin, respectively. Tetracycline was used at a concentration of 1 μg/mL for induction of YPEL3-V5.

After 15 days, the cells were stained with 1% crystal violet in 70% methanol for 5 minutes. Plates were washed with PBS for 5 minutes, colonies counted and then photographed. Each well was destained with 1 mL 10% acetic acid for 5 minutes and the absorbance recorded at 595nm.

Cell Viability Assay

U2OS-TetR cells were transduced with Lenti-YPEL3 or Lenti-LacZ, selected with Zeocin and then pooled populations of parental, YPEL3-infected or LacZ infected U2OS-TetR cells were plated onto 96 well plates (1000 cells per well). The next day indicated cells were treated with to 1 μg/mL tetracycline for an additional 24 hours after which the cells were refed with media containing 10% Cell Quanti-Blue reagent. Cells were incubated for 30 minutes after which the cell media was transferred to a black 96 well dish and fluorescence detected using a Safire microplate reader following manufacturer's recommendation (BioAssay Systems). Each treatment condition was assessed in quadruplicate after subtraction of fluorescence values from samples containing only media with 10% Cell Quanti-Blue reagent.

Senescence Associated beta-galactosidase Staining

Cells were processed with the Senescence beta-galactosdiase Staining Kit (Cell Signaling Technology) according to the manufacturer's instructions and visualized on an Olympus 1X70 fluorescence microscope.

Senescence Associated Heterochromatic Foci (SAHF) Analysis

To examine SAHF formation, cells which were previously subjected to beta-galactosidase staining were washed twice with DPBS, permeabilized with 0.2% TritonX-100/PBS for 10 minutes, stained with 25 μg/mL Hoechst dye for 5 minutes, and then washed twice with DPBS. Cells were examined under an Olympus 1X70 fluorescence microscope.

TissueScan Tumor Screen

TissueScan Ovarian Cancer Tissue qPCR Array HORT101 was purchased from OriGene. cDNA was rehydrated per manufacturer's instructions and RT-PCR was performed as described above except that the GAPDH Assay on Demand was multiplexed with the YPEL3 Assay on Demand (Applied Biosystems, validated targets).

5-azadeoxycytidine (5aza-dC) Treatment

A2780, Cp70 and C30 cell lines were plated at 150,000 per 10cm plate. After 24 hours, the media was replaced and the cells were treated with 5aza-dC at 0, 2.5, 5 and 10 μM

concentrations. Cells were refed with the appropriate dose of 5aza-dC every 24 hours for 5 days. Following 5 days of treatment, RNA was isolated as described above and quantified using the Nanodrop with 260/280 ratios ranging from 2 to 2.2. RT-PCR was then performed as described above. Error bars represent 95% confidence interval obtained from an individual experiment. These experiments were repeated in triplicate with similar results obtained. For CpG methylation sodium bisulfite conversion of genomic DNA was performed using EZ DNA Methylation Kit following manufacturer's protocol (Zymo Research). Retrogen performed DNA sequencing of Topo-cloned PCR products. Primers for CpG island PCR fragments A through D will be made available on request.

Results

YPEL3 is a p53-regulated gene

YPEL3 possessed a gene expression profile in MCF7 cells transfected with various combinations of siRNAs targeting Hdm2, HdmX and p53 consistent with it being a p53 target gene (10). To confirm that YPEL3 was in fact a p53-regulated gene, we first examined how endogenous YPEL3 mRNA and protein was affected by DNA damage. Increases in YPEL3 mRNA levels were seen in doxorubicin treated Hct116 colon carcinoma cells (Figure 1A) and 76Ntert immortalized mammary epithelial cells exposed to the radiomimetic bleomycin (Figure 1B). The DNA damage induction of YPEL3 was also observed at the protein level as an approximately 15kDa protein was increased 2 fold in doxorubicin treated Hct116 cells (Figure 1C). We believe this represents endogenous YPEL3 as Hct116 cells transduced with a shYPEL3 retrovirus results in loss of the protein (Figure 1C, shYPEL3). Additionally the level of YPEL3 mRNA induction was significantly reduced in doxorubicin treated Hct116 cells lacking p53 (Supplementary Figure 1B).

These findings are consistent with p53 activation of YPEL3 in human tumor cells possessing wild-type p53. Towards demonstrating that p53 directly induces the YPEL3 gene a 1.5 Kbp region of the YPEL3 gene spanning -1386 to +120 relative to the start site of transcription was cloned into a firefly luciferase reporter vector. Based on a bioinformatic screen (15), two putative p53 binding sites were identified, one 1.3 Kbp 5' of the YPEL3 promoter and a second immediately upstream of the YPEL3 promoter (Figure 2A). Cotransfection of the YPEL3-luciferase reporter with wild-type p53 in either Hct116-/-p53 or H1299 cells led to an increase in YPEL3 promoter activity (Figure 2B). Next, a deletion of the YPEL3-luciferase reporter was created effectively removing the far upstream p53 binding site. When this reporter YPEL3 (-485:+120)Luc was transfected into Hct116+/+ p53 cells, the addition of doxorubicin resulted in an increase in luciferase activity (Figure 2B). Finally, when a 50 bp region encoding the p53 binding sites was cloned into a luciferase reporter construct, p53 was able to activate the reporter in contrast to a scrambled 50-mer (open bars) or a 50-mer where critical p53 binding site nucleotides were mutated (gray bars; Figure 2C). Having established that the YPEL3 promoter could be activated by p53 when cloned into a plasmid reporter construct we next set out to test whether p53 protein associated with the YPEL3 promoter *in vivo*. p53 chromatin immunoprecipitation assays were performed with Hct116 cells undamaged (untreated) or damaged with doxorubicin. As expected, p53 was shown to bind *in vivo* to the YPEL3 promoter in DNA damaged Hct116 cells (Figure 2D).

YPEL3 induces growth inhibition by triggering cellular senescence

Murine YPEL3 (SUAP) has been found to inhibit cell growth and to induce programmed cell death in murine myeloid precursor cells (13). To test the biological impact of human YPEL3 we cloned the YPEL3 cDNA into a tetracycline inducible expression vector. MCF7 and U2OS cells expressing the TetR repressor protein were infected with lentivirus carrying the YPEL3 construct and placed under Zeocin selection. We added tetracycline to induce YPEL3

expression to a level comparable to the increase in endogenous YPEL3 mRNA observed following DNA damage (Figure 3C). Using a colony formation assay both cell lines showed considerably fewer colonies when expressing YPEL3 compared to cells not induced to express YPEL3 (Figure 3A/B). Growth suppression was also observed after shorter time periods of YPEL3 induction. When pooled populations of U2OS-TetR cells transduced with no construct (parental), LacZ or YPEL3 were induced for 24 hours with tetracycline, only the YPEL3 tetracycline treated U2OS cells showed a significant decrease in cell viability (Figure 3D).

Due to difficulties in long-term growth of YPEL3 expressing cells, the inability to detect apoptosis and observed morphological changes, we examined the possibility that induction of YPEL3 would trigger cellular senescence. Two hallmarks of cellular senescence in human cells are the detection of increased acidic beta-galactosidase activity (16) and the appearance of foci within the nuclei of senescent cells (senescent associated heterochromatin foci, SAHF) (17, 18). Parental, LacZ and YPEL3-V5 expressing U2OS-TetR cells were grown for 6-7 days in the presence or absence of tetracycline and then assayed for beta-galactosidase activity or the presence of SAHF nuclei. A clear increase (~38%) in cellular senescence was observed in U2OS/YPEL3-TetR cells exposed to tetracycline (Figure 4A/B). No increase in basal cellular senescence (~5%) was observed in parental or LacZ transduced U2OS cells exposed to tetracycline. Similar levels of senescence were observed based on SAHF analysis (Figure 4C/D). Induction of cellular senescence was also observed in MCF7/YPEL3-TetR cells (Supplementary Figure 2A) or when YPEL3 was transduced into IMR90 human diploid fibroblasts (Supplementary Figure 2B/C). These findings, together with the observation that YPEL3 gene is activated by p53, suggest that YPEL3 protein may represent a novel p53-senescent activator.

YPEL3 functions downstream of p53-dependent cellular senescence

In order to determine where YPEL3 fits within the senescence pathway, IMR90 cells were transduced with varying combinations of lentivirus expressing H-ras, GFP, YPEL3, shp53, shLacZ and shYPEL3. Seven days after transduction senescent cells were identified by beta-galactosidase activity (Figure 5A) or by SAHF (Figure 5B). As expected, H-ras (Figure 5 panels A and C) and YPEL3 (Figure 5 paneld D) triggered senescence in 80% of the transduced cells. The combination of H-ras and YPEL3 (Figure 5 panels E) did not result in an increase in senescent cells suggesting that the two proteins may function in the same pathway. The decrease in cellular senescence when H-ras was co-infected with an shRNA targeting YPEL3 suggests that YPEL3 is a critical target in ras mediated senescence (Figure 5 panels H). Finally, the shp53 block of H-ras premature senescence could be reversed by the addition of YPEL3 (Figure 5 panels F and G). This finding suggests that YPEL3 functions downstream of p53 signaling and leads us to propose that YPEL3 represents a novel p53-senescent activator. Similar experiments were performed using U2OS cells. Interestingly, while H-ras only induces approximately 20% of the U2OS cells to undergo senescence, YPEL3 is very potent in activating premature senescence in this tumor cell line (Supplementary Figure 3).

In experiments to confirm YPEL3 overexpression and knockdown we observed that H-ras induction did not trigger the expected increase in YPEL3 mRNA levels at day 7 post transduction (Supplementary Figure 4A, transductions A and C). However, when we followed YPEL3 gene expression of H-ras induced IMR90 cells on a daily basis, starting at day 6, we observed a cyclical expression pattern (Supplementary Figure 4B) for both YPEL3 and p21. This periodic induction of p21 mirrors that reported by Mason *et al.* for several known senescence inducible genes (19) suggesting that molecular targets for senescence, like YPEL3 and p21, are transiently induced as cells reprogram to a permanently arrested state.

YPEL3 gene expression is reduced in human tumors

Since YPEL3 is a p53-regulated gene with the ability to trigger cellular senescence in normal and tumor cells we reasoned that its expression should be downregulated in human tumors. In a screen of eight different human tumor types, a significant decrease in YPEL3 mRNA expression was observed in lung, colon and ovarian tumor samples relative to normal controls. In a larger screen of 30 ovarian tumors relative to 6 normal ovarian samples we observed a significant decrease in YPEL3 in the tumor samples (p-value < 0.012; Figure 6A). Analysis of the YPEL3 promoter uncovered a 950 bp CpG island, suggesting that YPEL3 downregulation maybe occurring through CpG hypermethylation. Consistent with this model the treatment of human ovarian cell lines harboring wild-type p53 (A2780), null for p53 (Cp70) or p53 mutant (C30) with increasing doses of 5-aza-deoxycytidine, a DNA methyltransferase inhibitor, produced a significant increase in YPEL3 gene expression (Figure 6B). Bisulfite treatment of genomic DNA from Cp70 cells treated with 5-aza-deoxycytidine, enabled us to identify a significant decrease in hypermethlyation of the YPEL3 CpG island (Figure 6C). The decreased expression of YPEL3 in both human tumors and human tumor cell lines provide further support that YPEL3 possesses tumor suppressor-type activity.

Discussion

The YPEL3 gene was first identified as SUAP, a small unstable apoptotic protein that appeared to be induced upon IL3 removal in a myeloid precursor cell line (13). Later SUAP received its current identification as YPEL3 due to it being one of five human genes with homology to the *Drosophila* Yippee protein (11). Our interest in YPEL3 originated from a microarray experiment in which we reactivated p53 in MCF7 cells by using RNAi approaches targeting Hdm2 and HdmX, negative regulators of p53 and observed an induction of YPEL3 gene expression (10). In the present study we provide data supporting YPEL3 as a novel p53-regulated gene. These findings are supported by the observation that YPEL3 appears to be a putative p53-regulated gene based on computational and microarray analyses (20). Using a variety of biochemical and molecular approaches we have demonstrated that YPEL3 is a p53 inducible gene (Figures 1 and 2). It is important to note that in the course of these studies we uncovered that YPEL3 is also induced by TA isoforms of p63 and p73 (A. Todd, personal communication). Given that YPEL3 activation leads to growth arrest (Figure 3) and is expressed in epithelial tissue (11), a tissue where p63 has important functional attributes, we are currently exploring the possibility that YPEL3 may play a role in p63 mediated differentiation of epithelial cells.

As mentioned previously, we anticipated that induction of human YPEL3 may trigger apoptosis but have been unable to demonstrate any consistent apoptotic response using subG1 or PARP cleavage indicators of programmed cell death. In contrast, our data strongly supports that the decrease in cell growth observed by colony formation or MTT based assays (Figure 3) results from the induction of cellular senescence (Figures 4,5; Supplementary Figures 3,4). We were able to trigger premature cellular senescence in primary cells and two tumor cell lines (U2OS, MCF7), using overexpression by viral transduction and controlled tet-regulated expression to induce a physiologically relevant expression. Since recent results indicate that Nutlin, a small molecule inhibitor of Hdm2:p53 association, can trigger reversible beta-galactosidase activity (21), cellular senescence was confirmed in these studies using both beta-galactosidase activity and the detection of senescent activated heterochromatin foci.

Several important findings regarding the signaling of senescence by YPEL3 were uncovered in this study. First, induction of YPEL3 alone is sufficient to trigger cellular senescence in all three cell lines studied (IMR90, U2OS and MCF7). Experiments are currently ongoing to determine whether other known senescence-related proteins within the p53 signaling pathway are required to be present during this YPEL3-initiated cellular senescence. Our data with

IMR90 and U2OS cells is also consistent with previous reports showing that the loss of p53 can block H-ras mediated cellular senescence (18). This has allowed us to demonstrate another critical finding, namely that YPEL3 could rescue cellular senescence when co-transduced with H-ras + shp53 expressing lentivirus. Taken with the fact that shYPEL3 could block H-ras mediated premature senescence (Figure 5H) we conclude that YPEL3 functions downstream of p53 signaling consistent with our demonstration that YPEL3 is a p53-regulated gene.

Finally, consistent with our model that YPEL3 represents a novel tumor suppressor gene, we have demonstrated in ovarian (Figure 6), lung (data not shown) and colon tumors (R. Tuttle, manuscript in preparation) that YPEL3 gene expression is reduced in tumor samples relative to normal tissue. In Cp70 ovarian cells the molecular basis of this downregulation appears to be the hypermethylation of a CpG island immediately upstream of the YPEL3 promoter (Figure 6C). The induction of YPEL3 mRNA expression in ovarian cell lines treated with the DNA methylase inhibitor 5-aza-deoxycytidine confirms that DNA hypermethylation can impact YPEL3 expression. Thus the combination of low doses of demethylating agents with standard chemotherapy treatments may represent an effective approach towards the reactivation of YPEL3 in human tumors and subsequent induction of the tumor cell senescence pathway.

Supplementary Material

Refer to Web version on PubMed Central for supplementary material.

Acknowledgments

We would like to thank Dr. David Hitch for his critical insights and helpful discussions and Nick Maiorano for technical assistance. This work is supported by the NCI (CA64430 to SJB).

References

1. Mihara M, Erster S, Zaika A, et al. p53 has a direct apoptogenic role at the mitochondria. Mol Cell 2003;11:577–90. [PubMed: 12667443]
2. Vousden KH, Prives C. Blinded by the Light: The Growing Complexity of p53. Cell 2009;137:413–31. [PubMed: 19410540]
3. Manfredi JJ. p53 and apoptosis: it's not just in the nucleus anymore. Mol Cell 2003;11:552–4. [PubMed: 12667439]
4. Ventura A, Kirsch DG, McLaughlin ME, et al. Restoration of p53 function leads to tumour regression in vivo. Nature 2007;445:661–5. [PubMed: 17251932]
5. Xue W, Zender L, Miething C, et al. Senescence and tumour clearance is triggered by p53 restoration in murine liver carcinomas. Nature 2007;445:656–60. [PubMed: 17251933]
6. Campisi J. Senescent cells, tumor suppression, and organismal aging: good citizens, bad neighbors. Cell 2005;120:513–22. [PubMed: 15734683]
7. Brown JP, Wei W, Sedivy JM. Bypass of senescence after disruption of p21CIP1/WAF1 gene in normal diploid human fibroblasts. Science (New York, NY 1997;277:831–4.
8. Pantoja C, Serrano M. Murine fibroblasts lacking p21 undergo senescence and are resistant to transformation by oncogenic Ras. Oncogene 1999;18:4974–82. [PubMed: 10490832]
9. Kortlever RM, Higgins PJ, Bernards R. Plasminogen activator inhibitor-1 is a critical downstream target of p53 in the induction of replicative senescence. Nat Cell Biol 2006;8:877–84. [PubMed: 16862142]
10. Heminger K, Markey M, Mpagi M, Berberich SJ. Alterations in gene expression and sensitivity to genotoxic stress following HdmX or Hdm2 knockdown in human tumor cells harboring wild-type p53. Aging 2009;1:89–108. [PubMed: 19946469]
11. Hosono K, Sasaki T, Minoshima S, Shimizu N. Identification and characterization of a novel gene family YPEL in a wide spectrum of eukaryotic species. Gene 2004;340:31–43. [PubMed: 15556292]

12. Roxstrom-Lindquist K, Faye I. The Drosophila gene Yippee reveals a novel family of putative zinc binding proteins highly conserved among eukaryotes. Insect Mol Biol 2001;10:77–86. [PubMed: 11240639]

13. Baker SJ. Small unstable apoptotic protein, an apoptosis-associated protein, suppresses proliferation of myeloid cells. Cancer Res 2003;63:705–12. [PubMed: 12566317]

14. Markey M, Berberich SJ. Full-length hdmX transcripts decrease following genotoxic stress. Oncogene. 2008

15. Hoh J, Jin S, Parrado T, Edington J, Levine AJ, Ott J. The p53MH algorithm and its application in detecting p53-responsive genes. Proc Natl Acad Sci U S A 2002;99:8467–72. [PubMed: 12077306]

16. Dimri GP, Lee X, Basile G, et al. A biomarker that identifies senescent human cells in culture and in aging skin in vivo. Proc Natl Acad Sci U S A 1995;92:9363–7. [PubMed: 7568133]

17. Narita M, Nunez S, Heard E, et al. Rb-mediated heterochromatin formation and silencing of E2F target genes during cellular senescence. Cell 2003;113:703–16. [PubMed: 12809602]

18. Serrano M, Lin AW, McCurrach ME, Beach D, Lowe SW. Oncogenic ras provokes premature cell senescence associated with accumulation of p53 and p16INK4a. Cell 1997;88:593–602. [PubMed: 9054499]

19. Mason DX, Jackson TJ, Lin AW. Molecular signature of oncogenic ras-induced senescence. Oncogene 2004;23:9238–46. [PubMed: 15489886]

20. Sbisa E, Catalano D, Grillo G, et al. p53FamTaG: a database resource of human p53, p63 and p73 direct target genes combining in silico prediction and microarray data. BMC bioinformatics 2007;8 (Suppl 1):S20. [PubMed: 17430565]

21. Huang B, Deo D, Xia M, Vassilev LT. Pharmacologic p53 activation blocks cell cycle progression but fails to induce senescence in epithelial cancer cells. Mol Cancer Res 2009;7:1497–509. [PubMed: 19737973]

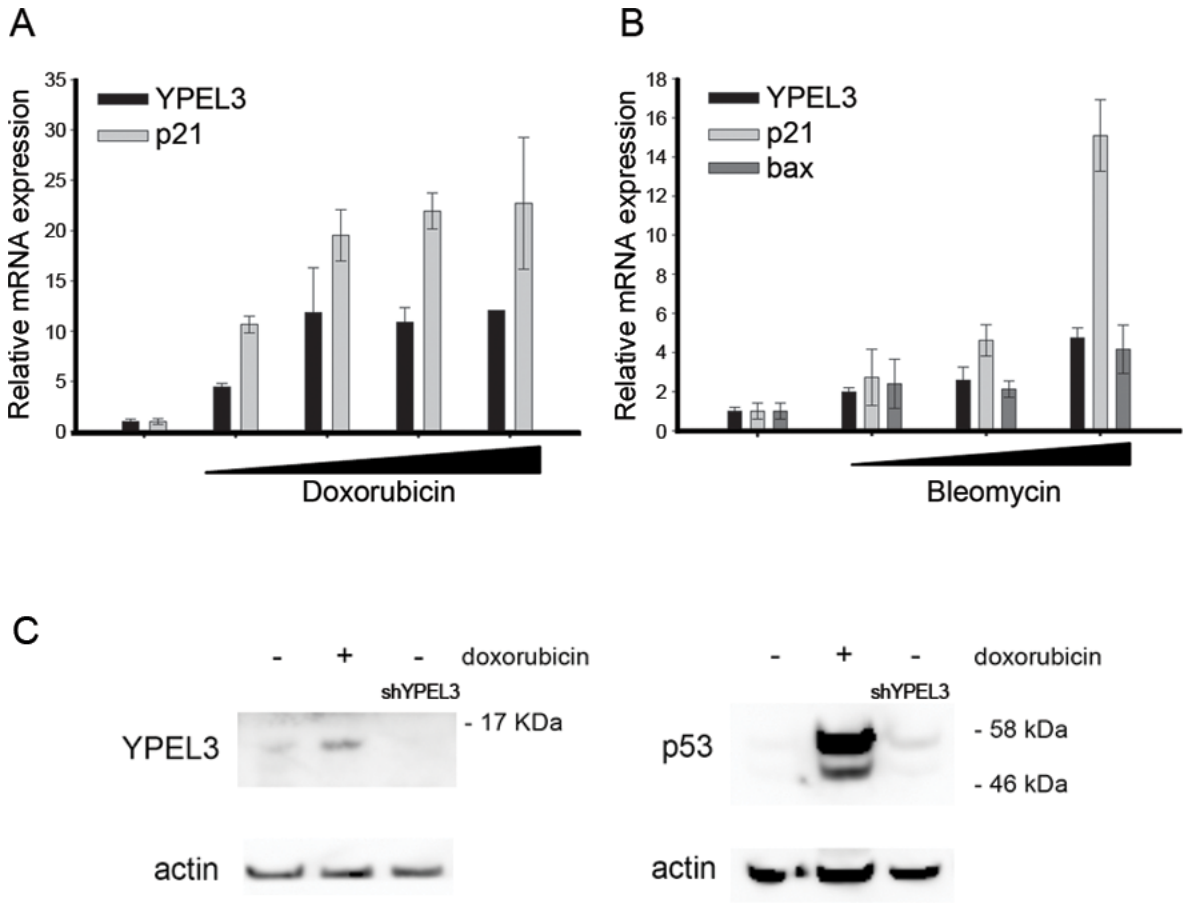

Figure 1.

YPEL3 increases in response to DNA damage. (A) Hct116+/+p53 cells were exposed to increasing doses of doxorubicin (0-0.5 μg/mL) or (B) 76NTert mammary epithelial cells exposed to bleomycin (0-0.1 units/mL) for 24 hours. YPEL3 and p21 mRNA levels were assayed by RT-PCR and normalized to GAPDH mRNA levels. Error bars represent 95% confidence intervals. (C) Endogenous YPEL3 (left panel) and p53 (right panel) protein levels increase in Hct116+/+p53 cells exposed to 0.4 μg/mL doxorubicin for 40 hours (compare untreated (-) to doxorubicin treated (+)). shYPEL3 represents Hct116+/+p53 cells transduced with a shYPEL3 expressing lentivirus.

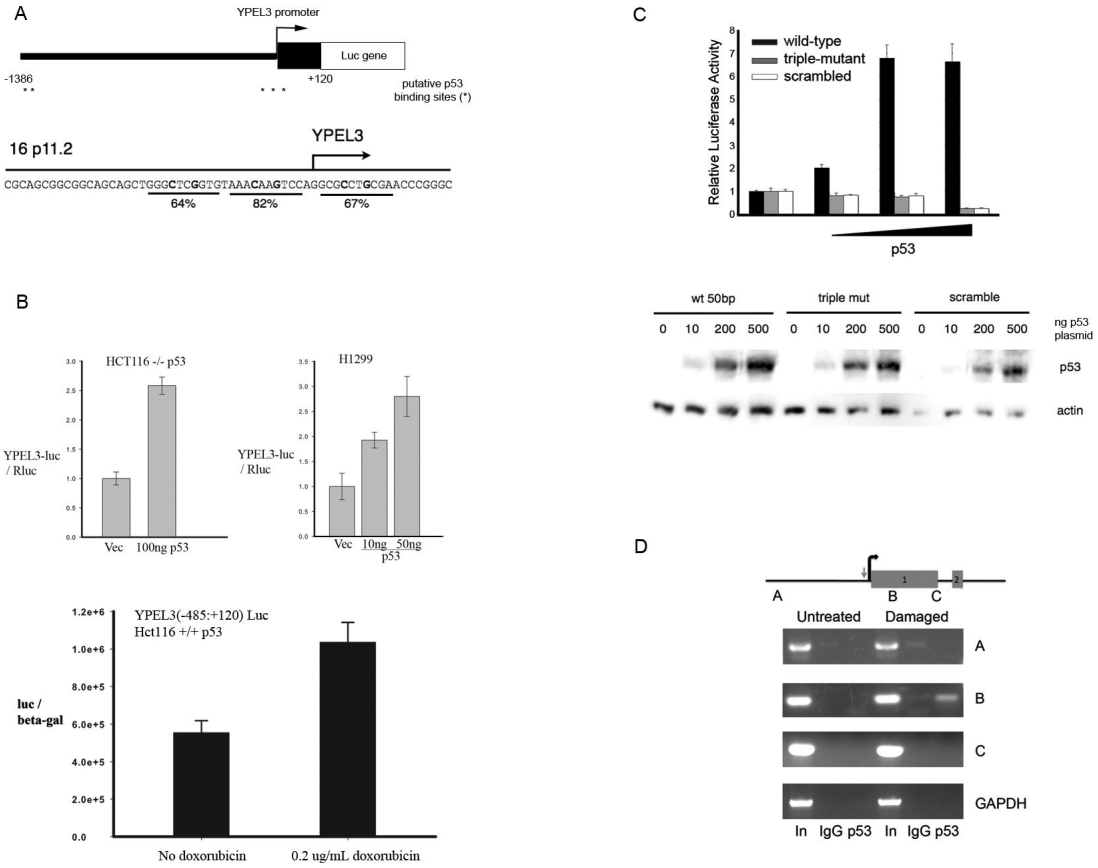

Figure 2.

YPEL3 is a p53-regulated gene. (A) A 1.5 kilobasepair region of the YPEL3 promoter spanning -1386 to +120 relative to the start site of transcription was cloned upstream of a firefly luciferase reporter gene (YPEL3-luc). The *s represent putative p53 half-sites as determined by TransFac analysis. Lower panel: location of the three p53 half sites with the percentage of conservation to the p53 consensus response half site. (B) YPEL3-luc activity was increased in Hct116-/- p53 (left panel) or H1299 (right panel) when cotransfected with a human p53 expression vector. YPEL3-luc luciferase activity was normalized by cotransfection with pCMV-Renilla-Luc and then performing dual luciferase assay for both firefly and renilla luciferase. Each assay was performed in triplicate (error bars are the standard error of the mean). Next, a truncation of region of the YPEL3 promoter spanning -486 to +120 was subcloned into the luciferase reporter vector used in A. The reporter was transfected into Hct116 cells harboring wild-type p53 and then subjected to DNA damage by doxorubicin treatment for 24 hours prior to firefly luciferase analysis. Normalization was performed by cotransfection with a pSV40-beta-galacosidase plasmid and then performing beta-galactosidase assays (C) A 50 bp region encompassing the region of the three putative p53 half sites near the YPEL3 promoter (black bars), a triple mutant where each half site harbored mutations at the critical C and G residues (grey bars) and a scrambled sequence (white bars) were cotransfected with increasing amounts of p53 plasmid. Lower panel shows the presence of p53 protein levels in all three sets of transfections. Relative luciferase activity represents firefly luciferase over renilla luciferase reading normalized to no p53 transfections (D) Chromatin immunoprecipitation assays were performed using undamaged or doxorubicin treated Hct116 +/+ p53 cells. Crosslinked chromatin was immunoprecipitated with p53 or IgG negative control antibodies. In: input chromatin that was reverse crosslinked. The PCR reactions were performed using primers specific to regions A,

B and C. PCR product A contains the putative upstream p53 binding site showing in (A). These primer sequences will be made available upon request.

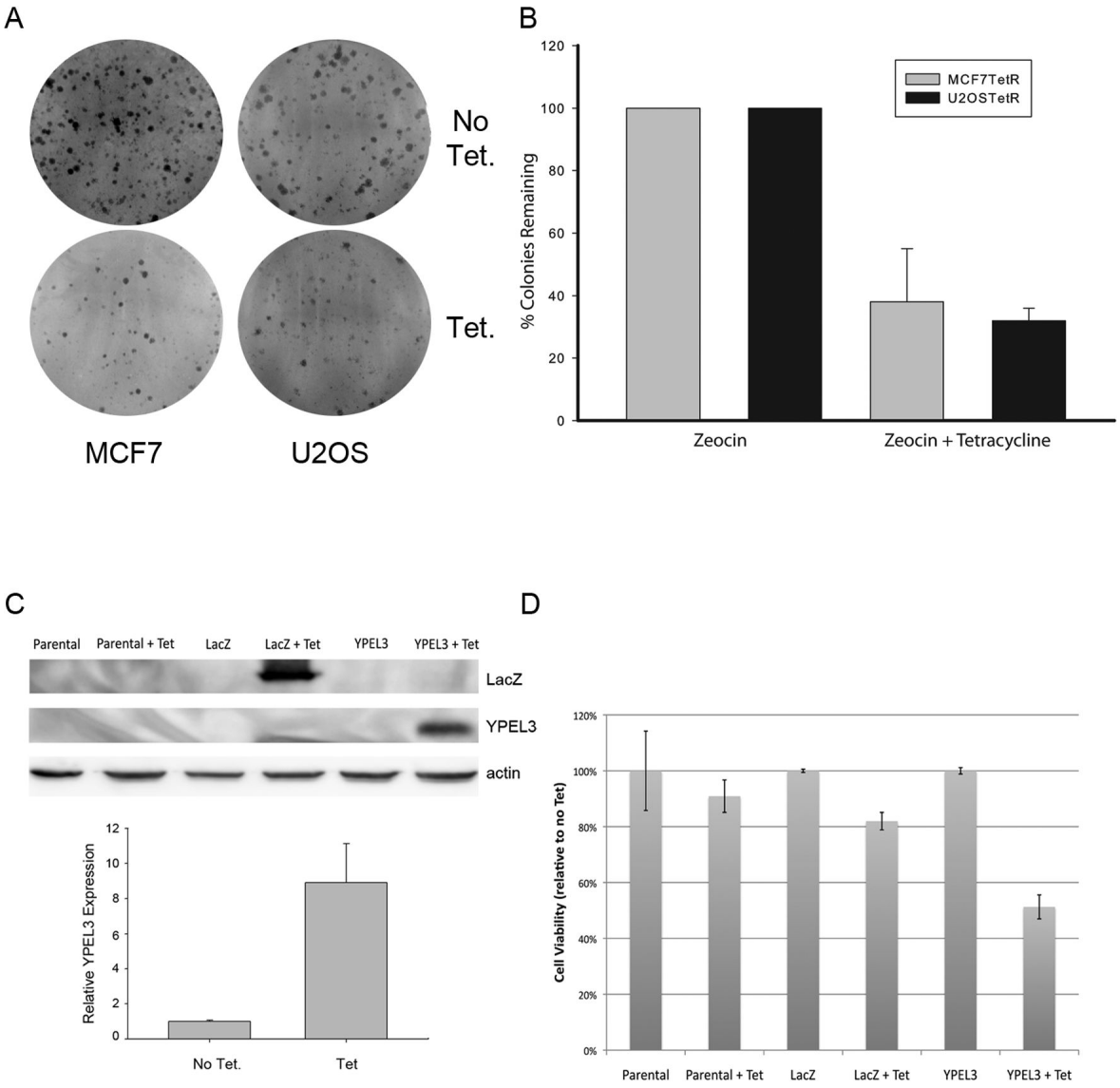

Figure 3.

Induction of YPEL3 leads to growth suppression. (A) Representative images of colony formation assays using MCF7TetR and U2OSTetR cells transduced with lentivirus containing a tet-inducible YPEL3-V5 cDNA, selected with Zeocin, and treated with and without 1 μg/mL Tetracycline (Tet). (B) Histograms of average colony numbers from colony formation assays were repeated in duplicate (U2OSTetR) or triplicate (MCF7TetR). Error bars represent the standard error of the mean. (C) Top: Western blot demonstrating YPEL3-V5 and LacZ protein expression in the indicated cell lines. Bottom: Q-RTPCR analysis of YPEL3 mRNA expression in MCF7TetR cells following treatment with tetracycline. (D) MTT assay of U2OSTetR cells transduced with the indicated lentivirus and then treated for 24 hours with or without tetracycline. Each condition was performed in quadruplet with error bars representing standard error of the mean.

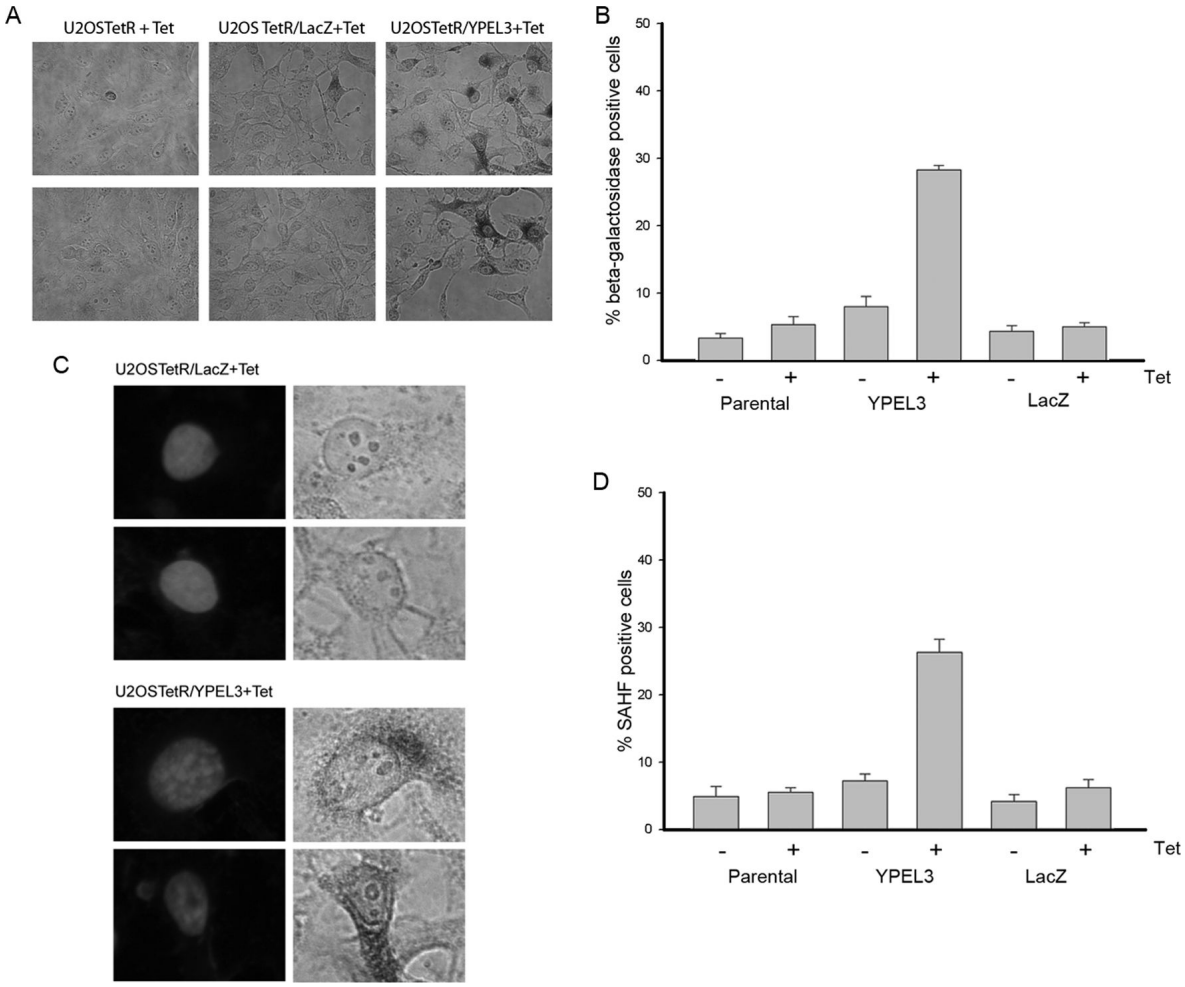

Figure 4.

YPEL3 induction triggers cellular senescence. (A/C) Representative images of U2OSTetR parental; U2OSTetR/LacZ and U2OSTetR/YPEL3 cells treated with 1 μg/mL Tetracycline for 6 days and subjected to SA-beta-galactosidase staining (A, 100X magnification) or subjected to Hoechst dye staining (C, 400X magnification). SA-beta-galactosidase staining (B) or SAFH analysis (D) was quantified for three independent experiments where a minimum of 100 cells was counted per treatment condition. The histrograms represent the average percentage of positive cells +/- standard error of the mean.

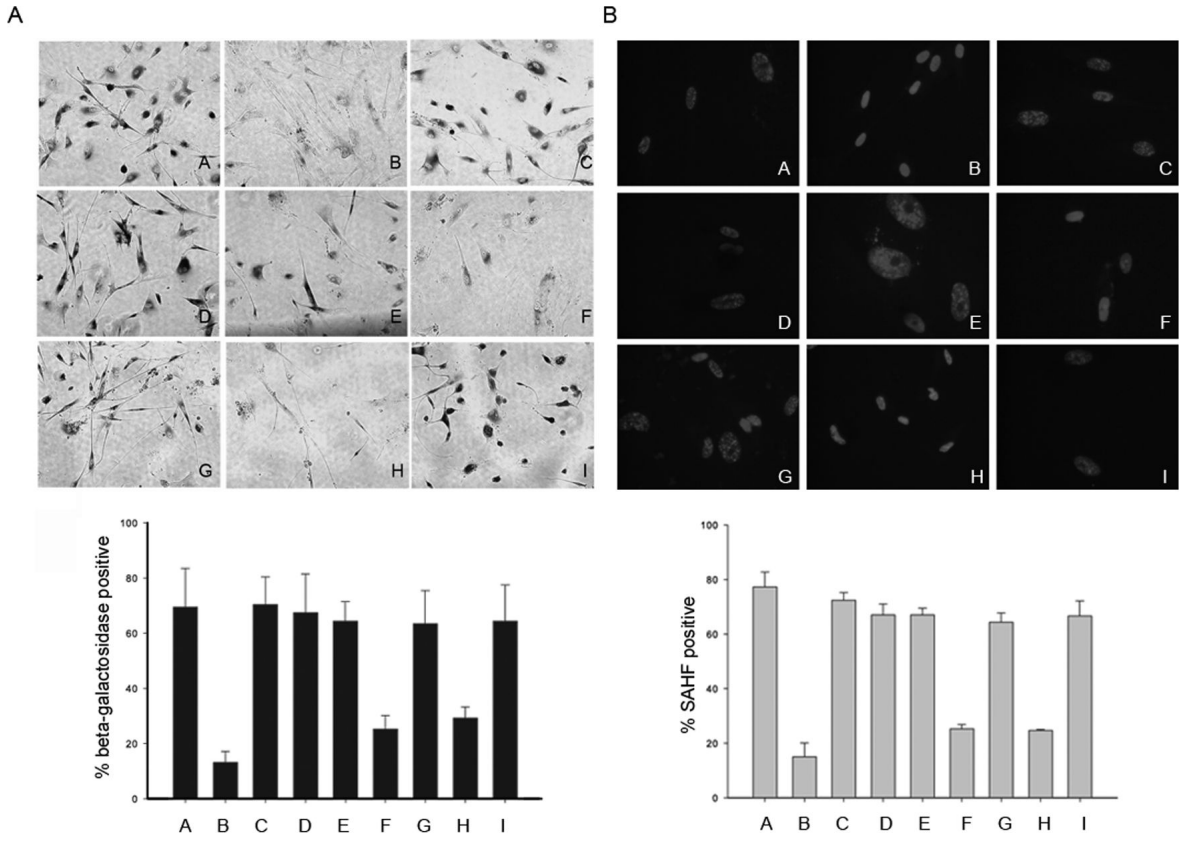

Figure 5.

YPEL3 functions downstream of p53 in ras-mediated premature senescence. IMR90 cells were transduced with A. H-ras, B. GFP, C. H-ras + GFP, D. YPEL3, E. H-ras + YPEL3, F. H-ras + shp53, G. H-ras + shp53 + YPEL3, H. H-ras + shYPEL3, I. H-ras + shLacZ and incubated under appropriate selection for 7 days. Cells were then subjected to SA-beta-galactosidase staining (A) or SAHF analysis by Hoechst dye staining (B). SA-beta-galactosidase images were captured at 100X magnification. SAHF images were captured at 400X magnification. Representative images from each treatment condition are shown. Histograms below images represent the average percentage of beta-galactosidase (A) or SAHF (B) positive cells from three biological replicate assays where a minimum of 100 cells was counted per treatment condition. Error bars represent the standard error of the mean.

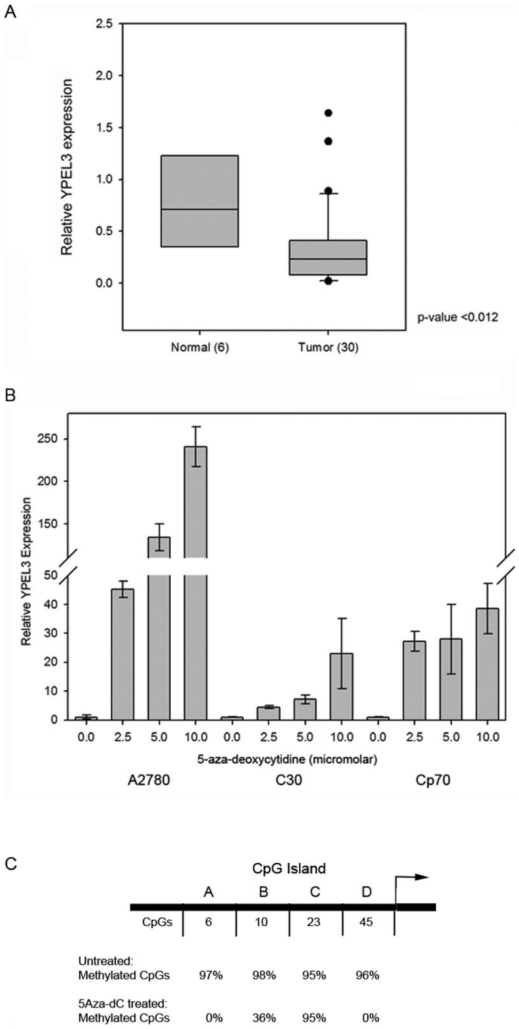

Figure 6.

YPEL3 expression is reduced in ovarian tumors and inhibition of CpG hypermethylation leads to increased YPLE3 mRNA in ovarian cell lines. (A) RT-PCR analysis of YPEL3 mRNA expression in 30 ovarian tumor and 6 normal ovarian samples obtained from Origene TissueScan Ovarian Cancer Array HORT101. (B) RT-PCR analysis of YPEL3 mRNA expression in platinum-sensitive ovarian cell line, A2780 and two cisplatin resistant ovarian cell lines, C30 and Cp70 after treatment with varying doses of 5-aza-deoxycytidine. (C) Analysis of CpG island upstream of YPEL3 promoter in 5-aza-dC treated Cp70 cells. PCR fragments (A-D) span -1222 to -8 relative to the start site of transcription. Bisulfite treated genomic DNA from treated (10 μM 5-aza-dC) or untreated Cp70 cells were used in PCR amplifications. Between 5-7 PCR inserts were DNA sequenced for each PCR fragment.